



3,5-Bis(2-fluorobenzylidene)-4-piperidone induce reactive oxygen species-mediated apoptosis in A549 cells

Guo-Yun Liu¹ · Cong-Cong Jia¹ · Pu-Ren Han¹ · Jie Yang¹

Received: 11 April 2017 / Accepted: 29 August 2017
© Springer Science+Business Media, LLC 2017

Abstract The presence of the substituents in the *ortho* position of the aromatic ring(s) is helpful to strengthen the biological activity, highlighting a so-called *ortho* effect. In this paper, we synthesized six mono-carbonyl curcumin analogs with the fluorine group, which imparts a variety of properties to certain medicines. Then, the cytotoxicity against A549 and NCI-H460 cells was evaluated by the MTT assay. The results exhibited that **1d** surfaced as an important lead compound displaying almost 13-fold cytotoxicity relative to curcumin against A549 cells. More importantly, **1d** was more stable and more massive uptake than curcumin, which may be relationship to their cytotoxicity, apoptotic activity and reactive oxygen species generation. The generation of reactive oxygen species is associated with falling apart in the redox buffering system, and subsequently induces lipid peroxidation, collapse of the mitochondrial membrane potential and ultimately leads to apoptosis. These data indicated that *ortho* effect and leading fluorine into medicine molecular are successful strategy to improve anticancer activity of mono-carbonyl curcumin analogs.

Keywords Curcumin analogs · Fluorine · Piperidone · Reactive oxygen species · Apoptosis

Introduction

Curcumin, a naturally occurring hydrophobic polyphenol abundantly found in turmeric, has attracted a particular interest in the area of cancer chemoprevention and chemotherapy (Reuter et al. 2008). In the last few decades, curcumin has been reported to influence multiple signaling molecules, such as protein reductase, cell survival protein, inflammatory molecules and so on, owing to its molecular structure and functionality (Gupta et al. 2011; Anand et al. 2008a, b). Chemically, curcumin contains electrophilic Michael acceptor pharmacophore, two hydroxyl groups, two methoxy groups and an active methylene Michael donor unit (Anand et al. 2011). However, high metabolic instability and low bioavailability significantly limit the clinical application of curcumin (Anand et al. 2007). This prompted interest in designing new analogs to improve the flaws (Mosley et al. 2007; Anand et al. 2008a, b). Among them, a series of diarylpentanoids with two identical aromatic ring region separated by five carbon spacers, has shown much more stability in vitro and improved pharmacokinetic profiles in vivo (Kudo et al. 2011; Yamakoshi et al. 2010; Liang et al. 2009; Ohori et al. 2006; Adams et al. 2004).

Drug candidates with one or more fluorine atoms have become commonplace. The chief advantage of fluorine, as fluoro-substituted aryl compounds, is that it imparts a variety of properties to certain medicines, including

Electronic supplementary material The online version of this article (<https://doi.org/10.1007/s00044-017-2056-x>) contains supplementary material, which is available to authorized users.

✉ Guo-Yun Liu
guoyunliu@126.com
✉ Jie Yang
yangjie1110@163.com

¹ School of Pharmacy, Liaocheng University, 1 Hunan Street, 252000 Liaocheng, Shandong, China

enhanced binding interactions, metabolic stability, changes in physical properties, and selective reactivity (Hagmann 2008). On the other hand, the position of the substituents on the aromatic ring(s) is critically important for their biological activity. For example, the presence of a *ortho* hydroxyl group strengthen significantly the cytotoxicity of cinnamaldehydes (Chew et al. 2010) and chalcones (Gan et al. 2013), and the potency of curcumin analogs in inducing phase II enzymes (Dinkova-Kostova et al. 2001). The phenomenon, the presence of the substituents in the *ortho* position of the aromatic ring(s) is helpful to strengthen the biological activity, is highlighting a so-called *ortho* effect. Our previous work (Dai et al. 2015; Liu et al. 2016) also reported that the “*ortho* effect” could obviously increase the cytotoxicity of the mono-carbonyl curcumin analogs. This also indicated that the “*ortho* effect” may be a successful strategy to improve the anticancer activity of mono-carbonyl curcumin analogs. Inspired by the above remarks, we design and synthesized six mono-carbonyl curcumin analogs with the presence of *ortho* fluorine group (Fig. 1). Further, we evaluated their cytotoxicity against human cancer cells using standard 3-(4,5-dimethylthiazol-2-yl)-2,5-diphenyltetrazolium bromide (MTT) assay and explored the apoptotic mechanism associated with curcumin analogs.

Materials and methods

Materials

Roswell Park Memorial Institute (RPMI)-1640 was from GIBCO. MTT, rhodamine 123, 2',7'-dichlorofluorescein diacetate, the reduced (GSH) and oxidized (GSSG) glutathione, glutathione reductase (GR), N-acetylcysteine (NAC), 2-vinylpyridine (97%), and thiobarbituric acid were obtained from Sigma. All other chemicals were of the highest quality available.

Synthesis of the curcumin analogs

General procedure for the synthesis of 1a–1e

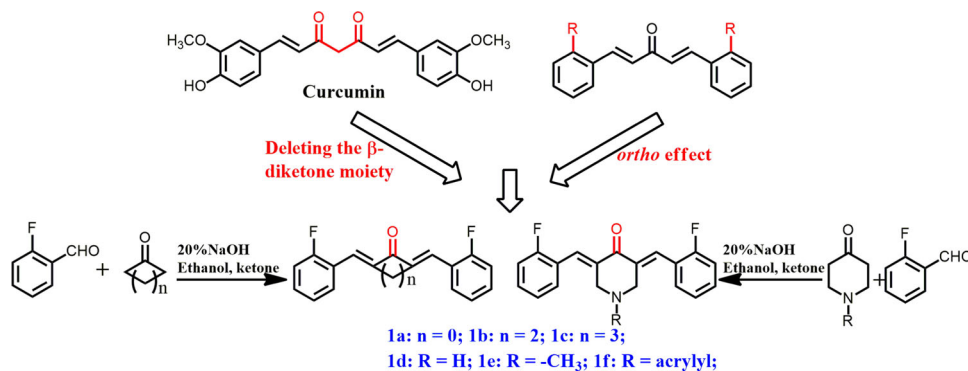
The mono-carbonyl curcumin analogs were synthesized according to the published procedure (Weber et al. 2005). Briefly, aqueous NaOH (20 wt%, 5 ml) was added dropwise to a vigorously stirred solution of 2-fluorine benzaldehyde (51 mmol) and ketone (actone, cyclopentanone, cyclohexanone, piperid-4-one, and 1-methylpiperid-4-one) (25 mmol) in ethanol (8 ml). After 24 h stirring at room temperature, distilled water (40 ml) was added to the reaction mixture followed by the neutralization with HCl. The precipitating yellow solid was filtered off, washed with distilled water and dried under vacuum. The crude products were directly charged onto a silica gel column and eluted with a mixture of ethyl acetate/petroleum to afford the pure product. Their structures were confirmed by ^1H and ^{13}C nuclear magnetic resonance (NMR) spectroscopy.

Synthesis of 3,5-bis(2-fluorobenzylidene)-4-piperidone (1f)

To a mixture of 3,5-bis(2-fluorobenzylidene)-4-piperidone (3.5 mmol) and K_2CO_3 (3.5 mmol) in acetone (10 ml) in an ice bath, acryloyl chloride (5.3 mmol) was added dropwise under stirring. The reaction was continued for 24 h at ambient temperature. After completion of the reaction, by monitoring with thin layer chromatography (TLC), the reaction mixture was poured into ice and extracted three times with EtOAc. The combined organic layers were washed with H_2O , then dried over Na_2SO_4 , and the solvent was removed in vacuo. The crude products were purified by silica gel column chromatography eluting with ethyl acetate/petroleum (Kia et al. 2013).

1,5-Bis(2-fluorophenyl)-penta-1,4-dien-3-one (1a) Yield: 71.4%; yellow solid; $R_f = 0.34$ (petroleum ether/EtOAc (10:1)); m.p. 65–69 °C; ^1H NMR (400 MHz, CDCl_3), δ 7.85

Fig. 1 Molecular structures of curcumin and its mono-carbonyl analogs



(d, $J = 16.4$ Hz, 2H, Ar-CH=C \times 2), 7.62 (dt, $J = 7.6, 1.6$ Hz, 2H, Ar-H⁶ \times 2), 7.37–7.42 (m, 2H, Ar-H⁴ \times 2), 7.12–7.23 (m, 6H, Ar-H³ \times 2, Ar-H⁵ \times 2, =CH-CO- \times 2); ¹³C NMR (100 MHz, CDCl₃), δ 189.0 (C, C=O), 162.9 (C, C-2), 160.4 (C, C-2), 136.1 (C, Ar-C), 131.9 (C, C-4), 129.4 (C, C-6), 127.6 (C, C-5), 124.5 (C, =CH-CO), 122.9 (C, C-1), 116.4 (C, C-3) (Liu et al. 2016, CAS: 914295-38-8).

2,5-Bis(2-fluorobenzylidene)-cyclopentanone (**1b**) Yield: 64.7%, light yellow solid; Rf = 0.25 (petroleum ether/EtOAc (8:1)); m.p. 204–207 °C; ¹H NMR 400 MHz (CDCl₃), δ 7.82 (s, 2H, Ar-CH=C \times 2), 7.57 (t, $J = 8.0$ Hz, 2H, Ar-H⁶ \times 2), 7.35–7.40 (m, 2H, Ar-H⁴ \times 2), 7.17 (t, $J = 8.0$ Hz, 2H, Ar-H⁵ \times 2), 7.12 (t, $J = 8.0$ Hz, 2H, Ar-H³ \times 2), 3.06 (s, 4H, CH₂-CH₂) ¹³C NMR (100 MHz, CDCl₃), δ 195.5 (C, C=O), 163.0 (C, C-2), 160.5 (C, C-2), 138.9 (C, Ar-C), 131.0 (C, =CH-CO), 130.1 (C, C-4), 125.7 (C, C-6), 124.0 (C, C-5), 116.0 (C, C-1), 115.8 (C, C-3), 26.5 (C, C-C) (Liang et al. 2009, CAS: 1158188-88-5).

2,6-Bis(2-fluorobenzylidene)-cyclohexanone (**1c**) Yield: 80.0%, yellow powder; Rf = 0.23 (petroleum ether/EtOAc (8:1)); m.p. 97–100 °C; ¹H NMR 400 MHz (CDCl₃), δ 7.83 (s, 2H, Ar-CH=C \times 2), 7.31–7.40 (m, 4H, Ar-H⁶ \times 2, Ar-H⁴ \times 2), 7.17 (t, $J = 8.0$ Hz, 2H, Ar-H⁵ \times 2), 7.09 (t, $J = 8.0$ Hz, 2H, Ar-H³ \times 2), 2.80 (t, $J = 4.0$ Hz, 4H, CH₂-CH₂-CH₂), 1.75–1.81 (m, 2H, CH₂-CH₂-CH₂); ¹³C NMR 100 MHz (CDCl₃), δ 189.6 (C, C=O), 162.1 (C, C-2), 159.6 (C, C-2), 138.2 (C, Ar-C), 130.7 (C, =CH-CO), 130.3 (C, C-4), 129.7 (C, C-6), 123.7 (C, C-5), 115.9 (C, C-1), 115.6 (C, C-3), 28.5 (C, CH₂-CH₂-CH₂), 23.0 (C, CH₂-CH₂-CH₂) (Liang et al. 2009, CAS: 1158188-80-7).

3,5-Bis(2-fluorobenzylidene)-4-piperidone (**1d**) Yield: 63.5%, light yellow solid; Rf = 0.25 (petroleum ether/EtOAc (1:1)); m.p. 138–142 °C; ¹H NMR 400 MHz (CDCl₃), δ 7.87 (s, 2H, Ar-CH=C \times 2), 7.34–7.40 (m, 2H, Ar-H⁶ \times 2), 7.26–7.29 (m, 2H, Ar-H⁴ \times 2), 7.16 (t, $J = 8.0$ Hz, 2H, Ar-H⁵ \times 2), 7.11 (t, $J = 8.0$ Hz, 2H, Ar-H³ \times 2), 4.04 (s, 4H, CH₂-NH-CH₂); ¹³C NMR 100 MHz (CDCl₃), δ 187.3 (C, C=O), 162.1 (C, C-2), 159.6 (C, C-2), 136.5 (C, Ar-C), 131.0 (C, =CH-CO), 130.9 (C, C-4), 128.9 (C, C-6), 123.0 (C, C-5), 116.0 (C, C-1), 115.8 (C, C-3), 48.1 (C-NH-C), 48.0 (C-NH-C) (Wu et al. 2013, CAS: 342808-40-6).

3,5-Bis(2-fluorobenzylidene)-1-methyl-4-piperidone (**1e**) Yield: 60.6%, yellow powder; Rf = 0.37 (petroleum ether/EtOAc (4:1)); m.p. 136–140 °C; ¹H NMR 400 MHz (CDCl₃), δ 7.90 (s, 2H, Ar-CH=C \times 2), 7.34–7.39 (m, 2H, Ar-H⁶ \times 2), 7.27 (t, $J = 8.0$ Hz, 2H, Ar-H⁴ \times 2), 7.17 (t, $J = 8.0$ Hz, 2H, Ar-H⁵ \times 2), 7.10 (t, $J = 8.0$ Hz, 2H,

Ar-H³ \times 2), 3.65 (s, 4H, CH₂-NH-CH₂), 2.41 (s, 3H, -CH₃); ¹³C NMR 100 MHz (CDCl₃), δ 186.0 (C, C=O), 162.1 (C, C-2), 159.6 (C, C-2), 134.7 (C, Ar-C), 130.9 (C, =CH-CO), 130.7 (C, C-4), 129.5 (C, C-6), 123.9 (C, C-5), 116.0 (C, C-1), 115.8 (C, C-3), 56.9 (C, CH₂-NH-CH₂), 45.5 (C, N-CH₃), (Wu et al. 2013, CAS: 1434133-36-4).

1-Acryloyl-3,5-Bis(2-fluorobenzylidene)-4-piperidone (**1f**) Yield: 65.8%, yellow powder; Rf = 0.42 (petroleum ether/EtOAc (1:1)); m.p. 121–124 °C; ¹H NMR 400 MHz (CDCl₃), δ 7.89 (d, $J = 16.0$ Hz, 2H, Ar-CH=C \times 2), 7.17–7.42 (m, 8H, Ar-H⁶ \times 2, Ar-H⁴ \times 2, Ar-H⁵ \times 2, Ar-H³ \times 2), 6.15–6.28 (m, 2H, CH=CH₂), 5.55 (dd, $J = 8.0, 4.0$ Hz, 1H, CH=CH₂), 4.66–4.85 (m, 4H, CH₂-NH-CH₂); ¹³C NMR 100 MHz (CDCl₃), δ 185.9 (C, C=O), 165.5 (C, CH₂-CH-C=O), 133.3 (C, C-2), 131.6 (C, Ar-C), 130.9 (C, =CH-CO), 130.7 (C, CH=CH₂), 130.4 (C, C-4), 128.9 (C, C-6), 126.5 (C, CH=CH₂), 124.3 (C, C-5), 122.4 (C, C-1), 116.0 (C, C-3), 46.6 (C-NH-C), 43.8 (C-NH-C) (Kia et al. 2013, CAS: 1428474-91-2).

Cell culture

Human lung cancer cells (NCI-H460) and human lung carcinoma cells (A549) were obtained from the Shanghai Institute of Biochemistry and Cell Biology, Chinese Academy of Sciences, and were cultivated in RPMI 1640 at 37 °C in a humidified atmosphere with 5% CO₂.

MTT assay

A549 and NCI-H460 cells were seeded at a density of 3×10^3 /well in 96-well plates and incubated for 24 h. Then cells were treated for another 48 h with compounds at the selected concentration before the MTT assay.

Stability assay

Stability of curcumin and **1d** (10 μ M) in RPMI 1640 supplemented with 10% (v/v) heat-inactivated fetal calf serum at 25 °C (The common international guideline for long-term stability studies specifies 25 ± 2 °C (ICH Harmonized Tripartite Guideline 2003)) was monitored at their band maximum for 120 min (at 10-min intervals) by using a multiwell-plate reader.

Cell apoptosis analysis

A549 cells (3×10^5 cells/well) were seeded into six-well plates. On the following day, the cells were treated with curcumin or **1d** for another 24 h. The treated cells were

collected and labeled with Annexin V-FITC/PI according to the manufacturer's instructions. A total of 5000 cells per sample were collected and analyzed by flow cytometry.

Intracellular reactive oxygen species (ROS) measurement

Intracellular ROS levels were determined according to 2',7'-dichlorofluorescein fluorescence assay as described previously (Liu et al. 2016). A549 cells (3×10^5 cells/well) were cultured in six-well and allowed to grow for 24 h. After 6 h of treatment with the test compounds in the absence or presence of GSH or NAC, A549 cells were incubated with 3 μ M DCFH-DA for 30 min at 37 °C in the dark. Then the cells were washed with PBS and analyzed immediately for 2',7'-dichlorofluorescein fluorescence intensity by flow cytometry.

Uptake and metabolic stability assay

A549 cells (3×10^5 cells/well) were seeded into six-well plates. On the following day, the cells were treated with curcumin or **1d** for 0.5, 1, 2, 4, or 6 h, followed by washing twice with ice-cold PBS. They were extracted with ice-cold methanol (1 ml/well) for 10 h at 4 °C. Then the suspension was centrifuged for 5 min (9400 \times g, at 4 °C), and the supernatant was then scanned using a UV/Visible spectrophotometer (Dai et al. 2015).

Measurement of GSH and GSSG levels

A microtiter plate assay for total GSH and GSSG content in A549 (3×10^5 cells/well) was performed by the glutathione reductase-DTNB recycling assay (Vandeputte et al. 1994), and the related details were described in our previous papers (Liu et al. 2016).

Determination of thiobarbituric acid-reactive substance

Lipid peroxidation was measured according to the protocol as described previously (Dai et al. 2015). A549 cells were cultured at a density of 3×10^5 cells/well in six-well and allowed to grow for 24 h. After treatment with the test compounds at the indicated concentrations for 15 h, A549 cells were harvested. Then the cells were resuspended in 200 μ l ice-cold water and lysed by three cycles of freezing and thawing. The absorbance of resulting supernatants was read at 532 nm, and lipid peroxidation was expressed as MDA equivalence (pmol MDA/mg protein)

Analysis of mitochondrial membrane potential

The mitochondrial membrane potential (MMP) was measured following the details described as our previous work (Dai et al. 2015). A549 cells (3×10^5 cells/well) were seeded into six-well plates and allowed to grow for 24 h. After 12 h of treatment with the test compounds in the absence or presence of GSH or NAC, A549 cells were incubated with 5 μ M Rhodamine 123 for 30 min at 37 °C and analyzed using a flow cytometry.

Statistical analysis

Data were expressed as the mean \pm SD of the results obtained from at least three independent experiments. Significant differences ($P < 0.05$) between the means of two groups were analyzed by Student's *t*-test.

Results and discussion

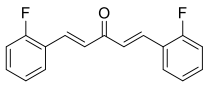
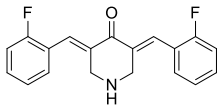
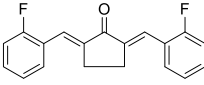
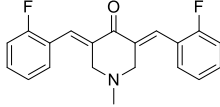
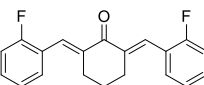
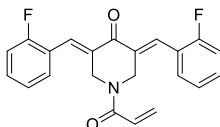
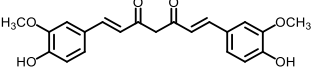
Synthesis

Compounds proposed in this work were synthesized employing a previously described procedure (Weber et al. 2005; Kia et al. 2013) (Fig. 1). **1a–1e** were synthesized via Aldol condensation from commercially available 2-fluorine benzaldehyde and different ketone at moderate to good yield (Fig. 1) after purification by silica gel column chromatography. **1f** was synthesized by **1e** and acryloyl chloride at room temperature under dry air until TLC analysis showed complete conversion (Kia et al. 2013). The desired product was obtained at 65.8% yield after silica gel filtration. All compounds were characterized by ^1H NMR and ^{13}C NMR.

Cytotoxicity and SAR

It has been reported that mono-carbonyl curcumin possesses a wide-spectrum of anti-cancer properties (Liang et al. 2009; Wu et al. 2013). The mono-carbonyl curcumin, containing a piperid-4-one structure, effectively inhibited the proliferation of prostate cancer cells and breast cancer cells (Adams et al. 2005). Therefore, MTT assays were used to assess the antiproliferative effect of curcumin and its analogs on A549 and NCI-H460 cancer cells. The IC_{50} values listed in Table 1 allowed us to identify the following SAR. (1) Almost all of the mono-carbonyl curcumin analogs with the *ortho* fluorine substituents were stronger than that of the leading curcumin. Especially, **1d** (3,5-bis(2-fluorobenzylidene)-4-piperidone) was about 13-times more active than curcumin against A549 cells. This result may be owing to the "*ortho* effect" and the much more stability of **1d** in RPMI 1640 supplemented with 10% (v/v) heat-

Table 1 Cytotoxicity of curcumin and its analogs against A549 and NCI-H460 cells.

Comps.	^a IC ₅₀ (μM)		Comps.	IC ₅₀ (μM)	
	A549	NCI-H460		A549	NCI-H460
 1a	17.0 ± 0.30	11.3 ± 0.70	 1d	4.2 ± 0.30	>100
 1b	>100	>100	 1e	12.6 ± 0.61	5.5 ± 0.27
 1c	30.5 ± 1.24	28.7 ± 1.87	 1f	7.4 ± 0.14	4.8 ± 0.37
 Curcumin	51.8 ± 2.6	41.0 ± 1.1			

^a The IC₅₀ value is the concentration of a compound tested to cause 50% inhibition of cell viability after 48 h of treatment, and is expressed as the mean ± SD for three determinations

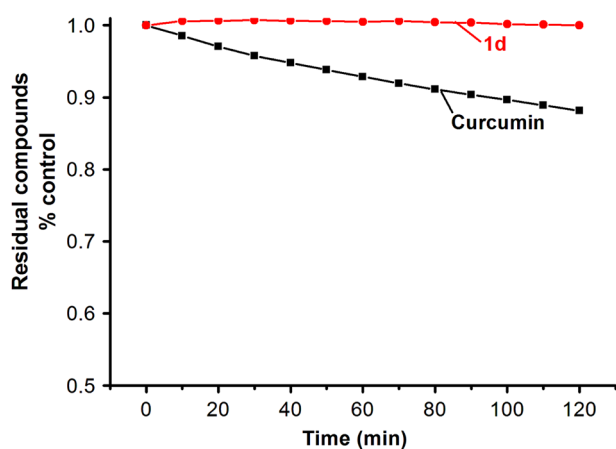


Fig. 2 Stability assessment on curcumin (10 μM) and **1d** (10 μM) in RPMI 1640 supplemented with 10% (v/v) heat-inactivated fetal calf serum at 25 °C by monitoring the decrease in their maximum absorbance

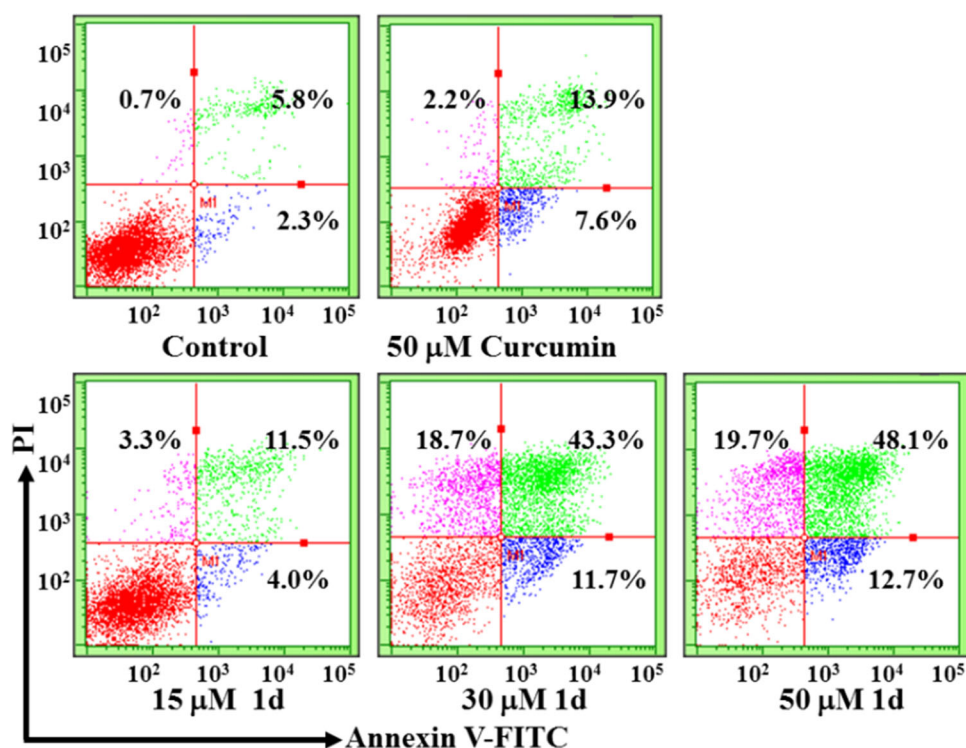
inactivated fetal calf serum than curcumin (Fig. 2). The strategy, deleting the β-diketone moiety could enhance the stability of curcumin, has been reported by Liang et al. (2009). (2) Notably, the compound **1d** exhibited the strongest cytotoxicity against A549 cells. This result may be related to

the 4-piperidone pharmacophore, which display a broad-spectrum of biological activity (Nunes et al. 2016), including anticancer, antimicrobial and anti-inflammatory. (3) More importantly, **1e** and **1f** showed potent cytotoxicity against A549 and NCI-H460 cancer cells. **1d** showed good inhibitory activity against A549 cells with low IC₅₀ value (4.2 μM), whereas low cytotoxicity against NCI-H460 cells with high IC₅₀ value (>100 μM). This phenomenon may be due to the 4-piperidone pharmacophore. Zou et al. (2016) also reported that **1d** was identified as selectively toxic to cancer cells. Therefore, **1d** was selected for further investigation of anti-cancer mechanisms against A549 cells.

Induction of apoptosis

It is known that apoptosis assay may provide important information to preliminary investigation of the mode of action. In the previous study (Zou et al. 2016), **1d** could induce the apoptosis of SGC-7901 and BGC-823 cells. Therefore, we detected the apoptosis-inducing activity of **1d** using flow cytometry. As illustrated in Fig. 3, **1d** was a potent inducer of apoptosis in the dose-dependent way. Treatment with 50 μM **1d** for 24 h resulted

Fig. 3 Flow cytometric analysis for apoptotic induction of A549 cells treated with curcumin and **1d** for 24 h. Each experiment was performed in triplicate



in 48.1% late apoptotic cells. This result suggest that the anti-cancer effect of **1d** is associated with the induction of A549 cell apoptosis.

Intracellular ROS generation

ROS generation has been implicated as an upstream signal that can trigger signaling transduction culminating in apoptosis (Pelicano et al. 2004). In the previous report (Wu et al. 2017), **1d** analog could induce apoptosis of lung cancer cell by promoting the generation of ROS. So, 2',7'-dichlorofluorescein diacetate (DCFH-DA) as a fluorescent probe was used to measure ROS generation. As shown in Fig. 4, **1d** caused a substantial increase in the ROS level in a dose-dependent fashion. Especially, **1d** induced significantly higher ROS accumulation than curcumin. More importantly, treatment with 30 μM **1d** for 6 h, the maximum ROS accumulation with a six-fold increase relative to the control. The high ROS-generation ability should be responsible for the better cytotoxicity of **1d**. The results also indicated that there may be a tight link among the ROS-generating ability, cytotoxicity and apoptosis-inducing activity. As expected, both GSH and NAC substantially reduced the ROS generation induced by 30 μM **1d** in A549 cells. The results further indicated that the ROS generation is the key regulator of **1d**-induced apoptosis and cytotoxicity.

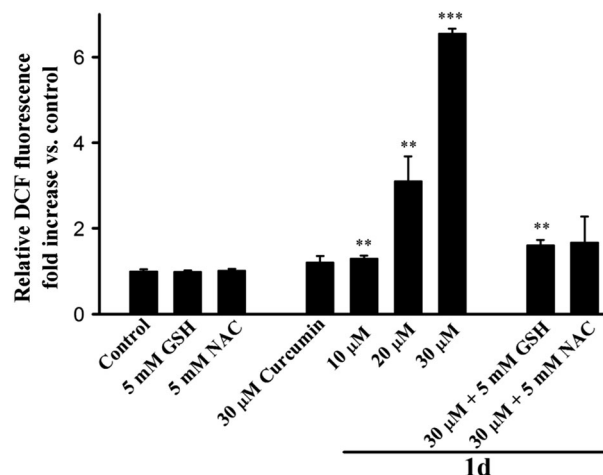


Fig. 4 Effects of GSH (5 mM) and NAC (5 mM) on the ROS generation induced by **1d** at the indicated concentrations against A549 cells. Each experiment was performed in triplicate

Cell uptake

The stability of mono-carbonyl analogs were greatly enhanced in vitro and their pharmacokinetic profiles were also significantly improved in vivo (Liang et al. 2009). The introduction of fluorine into a molecule can also enhance its metabolic stability (Hagmann 2008). We next compared the cellular uptake of **1d** and curcumin in A549 cells to explain the stronger cytotoxicity, ROS-generation ability and

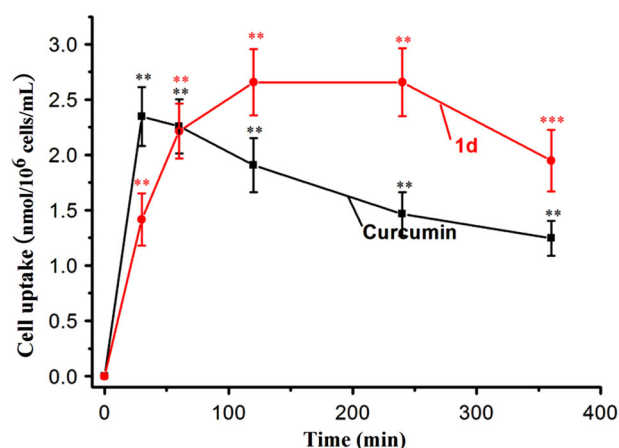


Fig. 5 Cellular uptake of curcumin and **1d** (30 μ M) estimated by absorbance measurement of methanol-extracted cell lysates as a function of the incubation period

apoptotic activity induced by **1d**. As illustrated in Fig. 5, curcumin was well absorbed to reach a peak value after 30 min of incubation, but it was rapidly metabolized for 6 h. Nevertheless, **1d** reached a peak value after 2 h of incubation and was fairly stable for 4 h. This result was in accordance with the ROS-generating ability and the cytotoxicity of curcumin and **1d**. It was also emphasized that incorporating of fluorine group and 4-piperidone pharmacophore into small molecules could effectively enhance its biological activity. Taken together, the higher uptake of **1d** may partly explain the better cytotoxic activity of **1d** than curcumin.

Determination of redox balance in NCI-H460 cell

A sustained flux of ROS usually resulted in an imbalance of intracellular redox state, which was estimated by the ratio of GSH and its disulfide GSSG (Klaunig and Kamendulis 2004). Adams et al. (2005) reported that **1d** significantly decreased the intracellular GSH content in HT29 human colon adenocarcinoma cells. Therefore, we tested the changes of the ratio of GSH and GSSG that induced by **1d**. As shown in Fig. 6, the ratios of GSH/GSSG were sharply decreased in a dose-dependent fashion after treatment with **1d** at the indicated concentrations. Especially, after treatment with 30 μ M **1d** for 6 h, the ratio of GSH/GSSG with a two-fold decrease relative to the control. This result indicated that **1d** not only elevated the ROS generation, but also disrupted the redox state of the A549 cells. Notably, a comparison of Fig. 4 with Fig. 6 clearly indicates that the ROS generation and collapse of intracellular redox buffering system induced by **1d** occur almost simultaneously. The results also indicated that there may be a relationship between the collapse of the redox buffering system and the ROS generation.

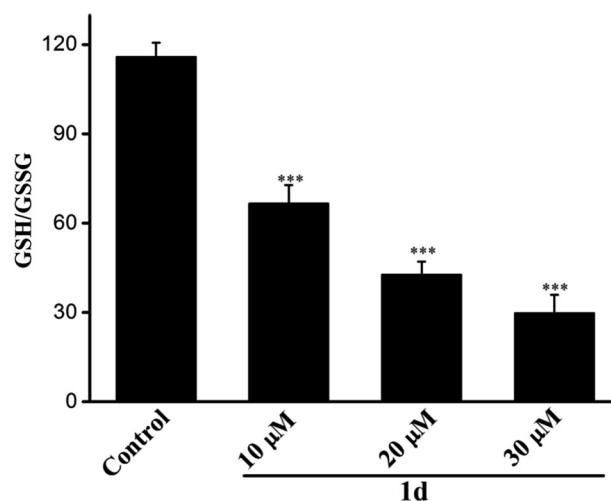


Fig. 6 The changes of GSH/GSSG ratios in A549 cells after treatment with **1d** at the indicated concentrations for 6 h. Each experiment was performed in triplicate

Lipid peroxidation

The major components of plasma membrane lipids are vulnerable to the attack of ROS and resulting in lipid peroxidation, which was increased as measured the amount of MDA. Combined **1d** and rapamycin could increase the level of lipid peroxidation product in tumor tissues (Chen et al. 2016). Exposure of the cells to **1d** at the indicated concentration for 15 h, we found that the malondialdehyde levels were significantly increased in a dose-dependent fashion (Fig. 7). This result also indicated that **1d** promoted the ROS generation. Especially, after treatment with 30 μ M **1d** for 15 h, the amount of MDA with about one-fold increase relative to the control.

The loss of MMP

Disruption of MMP is one of the earliest events in apoptosis (Lopez and Tait 2015). Curcumin has been demonstrated to induce mitochondrial depolarization (Morin et al. 2001). **1d** could also induce a depolarization of mitochondrial membrane potential in human breast cancer cells and human prostate cancer cells (Adams et al. 2005). In order to determined the involvement of mitochondrial in **1d** mediated apoptosis in A549 cells, we monitored the changes on mitochondrial membrane potential with Rhodamine 123 by flow cytometry. Exposure of the cells to **1d** and curcumin at the indicated concentrations, we found that **1d** was more active than curcumin in the collapse of mitochondrial membrane potential. It is a remarkable fact that **1d** exhibited perfect dose-dependent fashion (Fig. 8). These results indicated that treatment of **1d** against A549 cells triggers the loss of MMP. As expected, the addition of glutathione or N-

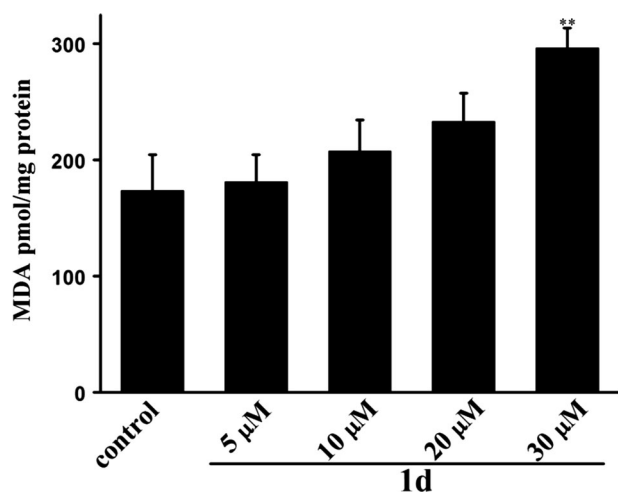


Fig. 7 MDA concentrations of A549 cells was determined after treatment with **1d** at the indicated concentrations for 15 h. Values are expressed as MDA equivalents (pmol)/ mg protein. Each experiment was performed in triplicate

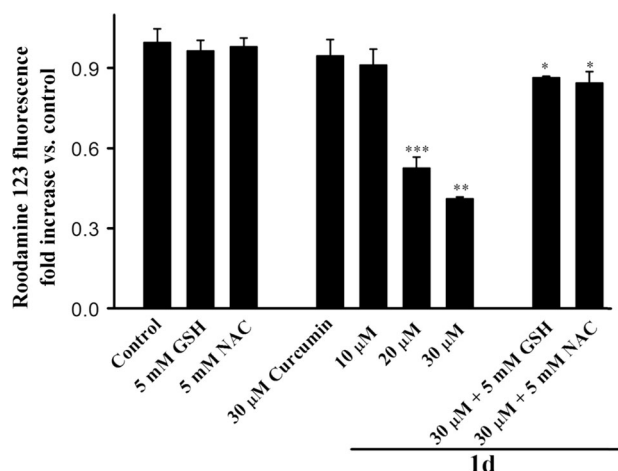
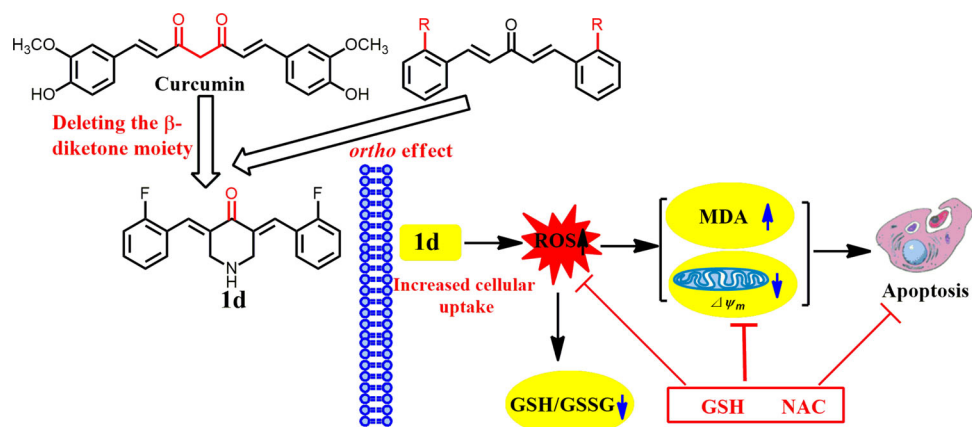


Fig. 8 Effects of GSH (5 mM) and NAC (5 mM) on the loss of mitochondrial membrane potential induced by **1d** at the indicated concentrations in A549 cells for 12 h. Each experiment was performed in triplicate

Fig. 9 Curcumin analog **1d** induce reactive oxygen species-mediated apoptosis in A549 cells



acetylcysteine remarkably blocked the loss of mitochondrial membrane potential induced by 30 μ M **1d**. The results also indicated that ROS production may be the upstream regulator in mitochondrial deficit.

Conclusions

In conclusion, we design and synthesized six mono-carbonyl curcumin analogs with the presence of *ortho* fluorine group, which imparts a variety of properties to certain medicines, and evaluated their cytotoxicity against A549 and NCI-H460 cells by the MTT assay. Compound **1d** surfaced as a potent lead compound displaying the most potent cytotoxicity. More importantly, **1d** showed good inhibitory activity against A549 cells, whereas low cytotoxicity against NCI-H460 cells. Mechanistic investigation reveals that the compound could effectively promote the ROS generation. The ROS generation is closely related with the imbalance of redox buffering system, and subsequently causes lipid peroxidation and loss of mitochondrial membrane potential, ultimately leading to cell apoptosis (Fig. 9). The more cytotoxic activity and ROS-generating ability of **1d** may be origin from its more stability, more massive uptake and the 4-piperidone pharmacophore. This work further indicated that *ortho* effect and incorporating of fluorine into medicine molecular are successful strategy to improve anticancer activity of mono-carbonyl curcumin analogs.

Acknowledgements This work was supported by the Doctoral Fund of LiaoCheng University (Grant No. 318051521, 318051424).

Compliance with ethical standards

Conflict of interest The authors declare that they have no competing interests.

References

- Adams BK, Ferstl EM, Davis MC, Herold M, Kurtkaya S, Camalier RF, Hollingshead MG, Kaur G, Sausville EA, Rickles FR (2004) Synthesis and biological evaluation of novel curcumin analogs as anti-cancer and anti-angiogenesis agents. *Bioorg Med Chem* 12:3871–3883
- Adams BK, Cai JY, Armstrong J, Herold M, Lu YJ, Sun A, Snyder JP, Liotta DC, Jones DP, Shoji M (2005) EF24, a novel synthetic curcumin analog, induces apoptosis in cancer cells via a redox-dependent mechanism. *Anti-Cancer Drugs* 16:263–275
- Anand P, Kunnumakkara AB, Newman RA, Aggarwal BB (2007) Bioavailability of curcumin: problems and promises. *Mol Pharm* 4:807–818
- Anand P, Sundaram C, Jhurani S, Kunnumakkara AB, Aggarwal BB (2008a) Curcumin and cancer: an “old-age” disease with an “age-old” solution. *Cancer Lett* 267:133–164
- Anand P, Thomas SG, Kunnumakkara AB, Sundaram C, Harikumar KB, Sung B, Tharakan ST, Misra K, Priyadarsini IK, Rajasekharan KN, Aggarwal BB (2008b) Biological activities of curcumin and its analogs (Congeners) made by man and mother nature. *Biochem Pharmacol* 76:1590–1611
- Anand P, Sung B, Kunnumakkara AB, Rajasekharan KN, Aggarwal BB (2011) Suppression of pro-inflammatory and proliferative pathways by diferuloylmethane (curcumin) and its analogs dibenzoylmethane, dibenzoylpropane, and dibenzylideneacetone: role of Michael acceptors and Michael donors. *Biochem Pharmacol* 82:1901–1909
- Chen WQ, Zou P, Zhao ZW, Chen X, Fan XX, Vinothkumar R, Cui R, Wu FZ, Zhang QQ, Liang G (2016) Synergistic antitumor activity of rapamycin and EF24 via increasing ROS for the treatment of gastric cancer. *Redox Biol* 10:78–89
- Chew EH, Nagle AA, Zhang Y, Scarmagnani S, Palaniappan P, Bradshaw TD, Holmgren A, Westwell AD (2010) Cinnamaldehydes inhibit thioredoxin reductase and induce Nrf2: potential candidates for cancer therapy and chemoprevention. *Free Radic Biol Med* 48:98–111
- Dai F, Liu GY, Li Y, Yan WJ, Wang Q, Yang J, Lu DL, Lin D, Zhou B (2015) Insights into the importance for designing curcumin-inspired anticancer agents by a prooxidant strategy: the case of diarylpentanoids. *Free Radic Biol Med* 85:127–137
- Dinkova-Kostova AT, Massiah MA, Bozak RE, Hicks RJ, Talalay P (2001) Potency of Michael reaction acceptors as inducers of enzymes that protect against carcinogenesis depends on their reactivity with sulfhydryl groups. *Proc Natl Acad Sci USA* 98:3404–3409
- Gan FF, Kaminska KK, Yang H, Liew CY, Leow PC, So CL, Tu LN, Roy A, Yap CW, Kang TS (2013) Identification of Michael acceptor-centric pharmacophores with substituents that yield strong thioredoxin reductase inhibitory character correlated to antiproliferative activity. *Antioxid Redox Signal* 19:1149–1165
- Goel A, Jhurani S, Aggarwal BB (2008) Multi-targeted therapy by curcumin: how spicy is it? *Mol Nutr Food Res* 52:1010–1030
- Gupta SC, Prasad S, Kim JH, Patchva S, Webb LJ, Priyadasini IK, Aggarwal BB (2011) Multitargeting by curcumin as revealed by molecular interaction studies. *Nat Prod Res* 28:1937–1955
- Hagmann WK (2008) The many roles for fluorine in medicinal chemistry. *J Med Chem* 51:4359–4369
- ICH Harmonized Tripartite Guideline, Q1A(R2) (2003) Stability testing for new drug substance and products
- Kia Y, Osman H, Kumar RS, Murugaiyah V, Basiri A, Perumal S, Wahab HA, Bing CS (2013) Synthesis and discovery of novel piperidone-grafted mono- and bis-spirooxindole-hexahydropyrrolizines as potent cholinesterase inhibitors. *Bioorg Med Chem* 21:1696–1707
- Klaunig JE, Kamendulis LM (2004) The role of oxidative stress in carcinogenesis. *Annu Rev Pharmacol Toxicol* 44:239–267
- Kudo C, Yamakoshi H, Sato A, Nanjo H, Ohori H, Ishioka C, Iwabuchi Y, Shibata H (2011) Synthesis of 86 species of 1, 5-diaryl-3-oxo-1, 4-pentadienes analogs of curcumin can yield a good lead in vivo. *BMC Pharmacol* 11:4. <https://doi.org/10.1186/1471-2210-11-4>
- Liang G, Shao L, Wang Y, Zhao C, Chu Y, Xiao J, Zhao Y, Li X, Yang S (2009) Exploration and synthesis of curcumin analogs with improved structural stability both in vitro and in vivo as cytotoxic agents. *Bioorg Med Chem* 17:2623–2631
- Liu GY, Zhai Q, Chen JZ, Zhang ZQ, Yang J (2016) 2,2'-Fluorine mono-carbonyl curcumin induce reactive oxygen species-mediated apoptosis in Human lung cancer NCI-H460 cells. *Eur J Pharmacol* 786:161–168
- Lopez J, Tait SW (2015) Mitochondrial apoptosis: killing cancer using the enemy within. *Br J Cancer* 112:957–962
- Morin D, Barthelemy S, Zini R, Labidalle S, Tillement JP (2001) Curcumin induces the mitochondrial permeability transition pore mediated by membrane protein thiol oxidation. *FEBS Lett* 495:131–136
- Mosley CA, Liotta DC, Snyder JP (2007) Highly active anticancer curcumin analogs. *Adv Exp Med Biol* 595:77–103
- Nunes LM, Hossain M, Varela-Ramirez A, Das U, Ayala-Marin YM, Dimmock JR, Aguilera RJ (2016) A novel class of piperidones exhibit potent, selective and pro-apoptotic anti-leukemia properties. *Oncol Lett* 11:3824–3848
- Ohori H, Yamakoshi H, Tomizawa M, Shibuya M, Kakudo Y, Takahashi A, Takahashi S, Kato S, Suzuki T, Ishioka C (2006) Synthesis and biological analysis of new curcumin analogs bearing an enhanced potential for the medicinal treatment of cancer. *Mol Cancer Ther* 5:2563–2571
- Pelicano H, Carney D, Huang P (2004) ROS stress in cancer cells and therapeutic implications. *Drug Resist Update* 7:97–110
- Reuter S, Eifes S, Dicato M, Aggarwal BB, Diederich M (2008) Modulation of anti-apoptotic and survival pathways by curcumin as a strategy to induce apoptosis in cancer cells. *Biochem Pharmacol* 76:1340–1351
- Vandeputte C, Guizon I, Genestie-Denis I, Vannier B, Lorenzon G (1994) A microtiter plate assay for total glutathione and glutathione disulfide contents in cultured/isolated cells: performance study of a new miniaturized protocol. *Cell Biol Toxicol* 10:415–421
- Wang Y, Xiao J, Zhou H, Yang S, Wu X, Jiang C, Zhao Y, Liang D, Li X, Liang G (2011) A novel monocarbonyl analog of curcumin, (1 E, 4 E)-1, 5-bis (2, 3-dimethoxyphenyl) penta-1, 4-dien-3-one, induced cancer cell H460 apoptosis via activation of endoplasmic reticulum stress signaling pathway. *J Med Chem* 54:3768–3778
- Weber WM, Hunsaker LA, Abcouwer SF, Deck LM, Vander Jagt DL (2005) Anti-oxidant activities of curcumin and related enones. *Bioorg Med Chem* 13:3811–3820
- Wu JZ, Zhang YL, Cai YP, Wang J, Weng BX, Tang QQ, Chen XJ, Pan ZE, Liang G, Yang SL (2013) Discovery and evaluation of piperid-4-one-containing mono-carbonyl analogs of curcumin as anti-inflammatory agents. *Bioorg Med Chem* 21:3058–3065
- Wu JZ, Wu SB, Shi LY, Zhang SS, Ren JY, Yao S, Yun D, Huang LL, Wang JB, Li WL, Wu XP, Qiu PH, Liang G (2017) Design, synthesis, and evaluation of asymmetric EF24 analogs as potential anti-cancer agents for lung cancer. *Eur J Med Chem* 125:1321–1331
- Yamakoshi H, Ohori H, Kudo C, Sato A, Kanoh N, Ishioka C, Shibata H, Iwabuchi Y (2010) Structure–activity relationship of C5-curcuminoids and synthesis of their molecular probes thereof. *Bioorg Med Chem* 18:1083–1092
- Zou P, Xia YQ, Chen WQ, Chen X, Ying SL, Feng ZG, Chen TK, Ye QQ, Wang Z, Qiu CY, Yang SL, Liang G (2016) EF24 induces ROS-mediated apoptosis via targeting thioredoxin reductase 1 in gastric cancer cells. *Oncotarget* 7:18050–18064